

Preparation and characterization of graphene oxide reinforced PVA film with boric acid as crosslinker

Jie Chen, Yadong Li, Yin Zhang, Yangguang Zhu

College of Chemistry, Chemical Engineering and Materials Science, Soochow University, Suzhou 215123, China

Correspondence to: Y. Li (E-mail: liyadong@suda.edu.cn)

ABSTRACT: PVA films were prepared through aqueous solution method, and boric acid (BA) as well as graphene oxide (GO) was added to improve the mechanical and thermal properties. It was found that 5 wt % BA could increase the tensile strength threefold (from 23.3 to 67.7 MPa), and the incorporation of 0.2 wt % GO would provide additional percentage growth of 30% (from 67.7 to 88.5 MPa). Moreover, an enhancement of thermal stability of PVA film was found when BA or GO filler was added. The reinforcement mechanisms of both BA and GO were investigated, and a competitive phenomenon that the addition of BA would influence the reinforcement effect of GO sheets was found. © 2015 Wiley Periodicals, Inc. *J. Appl. Polym. Sci.* **2015**, *132*, 42000.

KEYWORDS: biomaterials; composites; crosslinking; films; mechanical properties

Received 27 September 2014; accepted 16 January 2015

DOI: 10.1002/app.42000

INTRODUCTION

Polyvinyl alcohol (PVA), a production made from hydrolysis of polyvinyl acetate (PVAc), has been widely used in traditional industries, food and medical applications. Nowadays, researchers have given more and more attention to its utilization in medical field such as soft contact lenses, eye drops, slow release, tissue adhesion barriers, and artificial cartilage for the unique properties of nontoxicity, hydrophilicity, biocompatibility, and biodegradability. However, the relatively low mechanical strength, sensitivity to humidity and water-solubility limits its further use. To resolve the problems listed above, plenty of work has been done and lots of solutions have been proposed. Among them, crosslinking has been proved an effective way to improve the specific properties.²

For PVA, there are numerous kinds of crosslinking agents proved effective to enhance the mechanical properties, and in this article, we used boric acid (BA) to crosslink PVA. The reason BA was chosen instead of other reported crosslinkers such as hexamethylene diisocyanate,² glutaraldehyde (GA),^{3,4} or sulfosuccinic acid (SSA)⁵ is that, as an inorganic reagent, BA shows relatively low toxicity. What's more, many studies identified that the existence of certain concentration of BA exhibited beneficial biological properties, which would be helpful for angiogenesis and wound repair, metabolic system, bone strength and compositions of plasma and bone.^{6–12} Moreover, the boron concentration can maintain in a relatively narrow range in human body because it can be rapidly excreted in urine, which would prevent the accumulation in tissue or plasma, and sequentially minimize the toxicity.

At the same time, graphene, a monolayer of sp_2 -hybridized carbon atoms arranged in a two-dimensional lattice, has aroused increasing research interest recently due to its outstanding thermal, mechanical, electrical, and biological properties. These properties provide it with the potentials to be used in the field of electrode,¹³ biosensors,¹⁴ drug delivery,¹⁵ and polymer nanocomposites.¹⁶ Therefore, aside from crosslinking the PVA with BA, graphene-involved composites are also appropriate candidates to further improve the mechanical properties, since the addition of reinforcement materials is always believed a feasible and useful way to enhance a certain property of the matrix.^{17,18} A large amount of literatures have confirmed the efficacy of graphene in respect of improving the tensile strength,¹⁹ hardness,²⁰ wear resistance, and so on.²¹

Nevertheless, there still remain lots of problems arising with the tendency towards aggregation and processing difficulty. The strong interlayer cohesive energy and surface inertia of nanoscale graphene sheets makes it very difficult to disperse them homogeneously or orderly in polymer hosts. So, generally, the graphene needs to be modified before use. Another way to deal with the challenge mentioned above is to utilize graphene oxide (denoted as GO) instead. Since GO shares the parallel advantages like excellent mechanical property and biocompatibility but eliminates the disadvantages. With a range of reactive oxygen functional groups located on both edges and basal plane (such as epoxy and hydroxyl), GO exhibits great hydrophilicity and can provide a potential platform for the preparation of functionalized graphene.²² Herein, to simplify the process and



Figure 1. Photographs of (a) 9 wt % PVA aqueous solution with GO concentrations from 0.02 to 0.5 wt %, (b) TEM images of the GO sheets. [Color figure can be viewed in the online issue, which is available at wileyonlinelibrary.com.]

to attain the effect expected, GO was chosen as reinforced filler to prepare PVA/GO composite films in this paper.

So far, however, little work has been done to study the effect of BA on the mechanical or thermal properties of PVA film, and literatures about the combined effect of BA and GO are even less. Therefore, in this work, GO reinforcement combined with BA crosslinking was adopted. The reinforcement mechanism of both boric acid and GO filler was given and a competitive effect of these two components on the matrix was found. The possible mechanism that caused this competitive effect was investigated and a reasonable explanation was provided.

EXPERIMENTAL

Materials and Stable GO/PVA Suspensions

In this work, polyvinyl alcohol (denoted as PVA 124, Sino-pharm Chemical Reagent) with a degree of saponification of 98.0–99.8% was used. The polymerization degree is 2400–2500. Boric acid (denoted as BA, Shanghai Chemical Reagent) was used as a crosslinking agent. Graphene oxide (denoted as GO, Suzhou Dingan Technology) was used as a reinforcing filler. All other reagents involved in this study were of analytical grade and were used without further purification.

Figure 1(a) shows the photographs of 9 wt % PVA aqueous solution with GO concentrations from 0.02 to 0.5 wt %. When PVA was dissolved in deionized water completely, the solution was colorless and transparent. The color of the solution became brown-yellow after 0.02 wt % GO was added. With the increase of GO content, the color became black and the transparency was reduced. In addition, the concentration of GO also had a dramatic effect on the viscosity of the PVA solutions: the increasing content of GO developed a notably increase in viscosity, which showed a similar influence as BA. High viscosity always meant low fluidity, which could affect the thickness and homogeneity of the PVA/GO composite films. Figure 1(b) gives a typical TEM image of GO sheets, the fully exfoliated GO sheets are observed and rumples formed due to thin thickness are also noticed.

To further investigate the morphology and size distribution of the GO powders, AFM and SEM analyses were also conducted, as shown in Figure 2(a,b). From the AFM image, although some sheets overlapped with each other, we can still find that the sheets have heights of about 0.8 nm, which is characteristic of a fully exfoliated GO sheet. The size of the sheet marked by

the white symbols is about 0.5 μm . The SEM image exhibits a similar result of the shape and size of GO sheets: most of the sheets have lengths of 1–2 μm , and widths of about 0.5 μm .

Synthesis of cPVA and GO/cPVA Composite Films

The fabrication process of PVA film crosslinked by BA (denoted as cPVA) was as below. To exam the impact concentration of BA, different contents of BA (0, 2, 5, 8, 10, 15 wt % to the mass ratio of PVA) were added into 45.5 g deionized water. After the dissolution of BA, 4.5 g PVA was dissolved in BA solution at 90°C with a vigorously magnetic stirring to ensure the homogeneity. Prior to use, the prepared PVA aqueous solution stood for one night to remove the bubbles. A glass plate (75 mm \times 25 mm \times 1.5 mm) was dipped into the obtained solution. When the excessive liquid was excluded, the films were dried in room temperature for 6 h. After that, the cPVA films were peeled off the glass plate for the subsequent testing.

The procedure to prepare GO reinforced PVA composite film crosslinked by BA (denoted as cPVA/GO film) was as follows. The 9 wt % PVA aqueous solution with 5 wt % BA was used in this system. Various contents (0, 0.02, 0.05, 0.1, 0.2, 0.5 wt % with respect to the mass of PVA) of GO sheets were added into the as-prepared PVA aqueous solution with an ultrasonic treatment for 10 min. The cPVA/GO films were prepared in a way similar to that of the cPVA films. The PVA/GO films without BA as control group were also prepared with the same procedure.

Figure 3(a) shows the cPVA/GO films prepared from the solutions with GO concentrations from 0.02 to 0.5 wt %. It was found that when GO content increased, the thickness of the film increased accordingly (from 10 to 30 μm). In particular, the color of 0.5 wt % GO/PVA was darker than the others not only because of the higher GO concentration but also because the thickness increased. The inhomogeneity caused by low fluidity of PVA solution can also be certified in the sample of cPVA/0.5 wt % GO film, which was showed in Figure 3(b).

CHARACTERIZATION

Transmission electron microscopy (TEM, JEM-2100F, Japan Electron Optics Laboratory) was used to characterize the morphology and structure of GO sheets with an accelerating voltage of 200 kV. The GO sheets were dispersed in water with ultrasonication and then dropped onto copper grids before observation. Atomic force microscopic (AFM, MultiMode-8, Bruker)

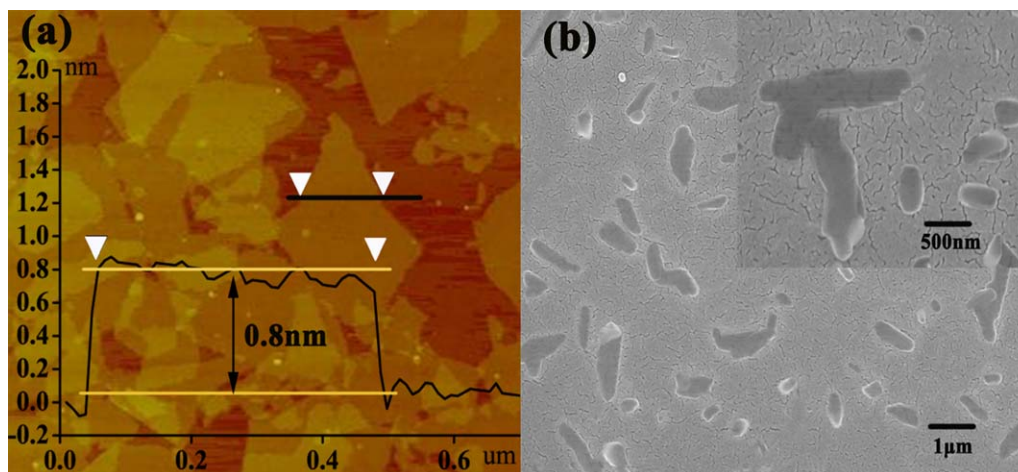


Figure 2. AFM image (a) and SEM (b) image of GO sheets. [Color figure can be viewed in the online issue, which is available at wileyonlinelibrary.com.]

images were taken out in a tapping mode to determine the thickness and size of GO sheets. The size distribution of GO sheets as well as the fractured surface of cPVA and cPVA/GO films was observed using scanning electron microscope (FE-SEM, S-4700, Hitachi). All samples were sputtered with gold before test.

GO, PVA, cPVA, and cPVA/GO composites were studied by X-ray diffraction (XRD, Rigaku D/Max) using Cu-K ($\lambda = 0.15406$ nm) radiation in a step-scan mode in the 2θ range $5\text{--}45^\circ$. GO was tested as powder, PVA and PVA/GO composites were analyzed as films.

Fourier transform infrared (FTIR) spectra of GO, PVA, cPVA, and cPVA/GO films were obtained using a FTIR spectrometer (IRPrestige-21). The FTIR spectra were collected over 32 scans in the $4000\text{--}500$ cm^{-1} region using the attenuated total reflectance mode at a resolution of 2 cm^{-1} . GO was mixed with KBr powders and pressed into tablets before characterization. Two parallel runs were done in the case of each sample.

Thermo gravimetric analysis (TGA) was carried out using a thermo-analyzer instrument (Diamond 5700 DSC, USA) to investigate the thermal stability of the materials. The test temperature was set from 20 to 800°C at a linear heating rate of $10^\circ\text{C min}^{-1}$ under a nitrogen flow (60 mL min^{-1}). Two parallel runs were done in the case of each sample.

The tensile strength and elongation at breaking were measured according to the Chinese standard method (GB 13022-91) with a WD-20D electronic universal testing instrument (Shenzhen Kejali Technology) at a crosshead speed of 50 mm min^{-1} . The tensile strength was calculated using the equation:

$$\sigma_t = \frac{p}{b \times d}$$

where σ_t is the tensile strength (MPa), p is the load at fracture (N), b is the sample width (mm), and d is the sample thickness (mm). Eight parallel runs were done in the case of each sample to get the average and standard deviations. The measurements were carried out under the following conditions: room temperature, initial length of 25 mm, initial width of 20 mm and thickness of $10\text{--}30$ μm . The thickness of films was measured using a thickness gauge (SD-201) with 0.001 mm measurement accuracy.

RESULTS AND DISCUSSION

Crosslink Reaction of PVA with Borate Ion

The mechanism of crosslink reaction of PVA with borate ion is suggested to be a didiol type, in which two diol units of PVA with one borate ion form a crosslink.^{23,24} The reaction process is divided into two steps, i.e., monodiol complexation step (1) and a crosslink reaction step (2) as shown by the equations in Figure 4. The number of crosslinks may be well controlled by

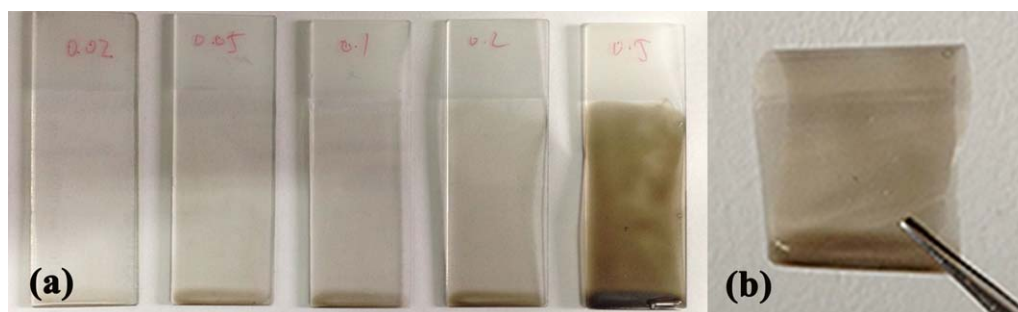


Figure 3. Photographs of (a) cPVA/GO films fabricated from the solutions showed above, (b) cPVA/0.5 wt % GO film peeled off the glass. [Color figure can be viewed in the online issue, which is available at wileyonlinelibrary.com.]

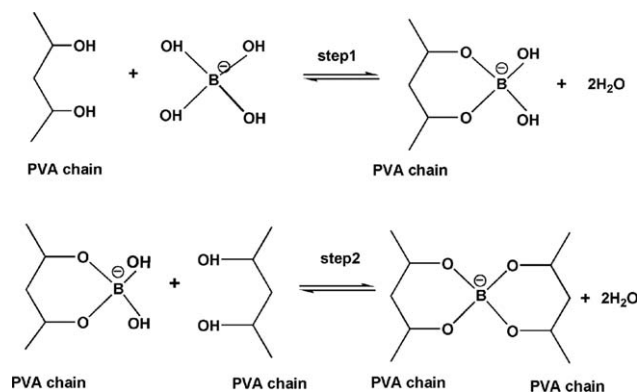


Figure 4. Illustration of crosslinking process of PVA and boric acid.

BA, polymer concentrations and reaction temperature, i.e., within a certain range of the ratio, the more BA is added, the more crosslinks are formed.^{24–27} The degree of crosslinking in the system, in contrast, decreases as the reaction temperature rises.^{27,28}

FTIR Spectrum

The FTIR spectrum (shown in Figure 5) of GO shows several characteristic peaks of various functionalities including C–O (ν C–O, 1080 cm^{-1}), C–OH (ν C–OH, 1262 cm^{-1}), C=O (ν C=O, 1758 cm^{-1}), and O–H (ν O–H, 3421 cm^{-1}). The peak at 1639 cm^{-1} is assigned to the adsorbed water. The main characteristic peaks of PVA can be identified as follows. The broad and strong absorption at 3100–3600 cm^{-1} is attributed to the symmetrical stretching vibration of hydroxyl in PVA. The peaks at 2800–3000 cm^{-1} are due to $-\text{CH}_2$ and the bands at 1000–1200 cm^{-1} are attributed to the stretching vibration of C–O. Compared with the pure PVA films, the crosslinked PVA samples show a slightly different spectrum. A new absorption peak appears at about 1030 cm^{-1} , which is believed to be caused by the bonding of B–O–C.^{29,30} Therefore, from the FTIR spectrum it is confirmed that B–O–C bonds are formed indicating that the reaction occurs between BA and PVA.

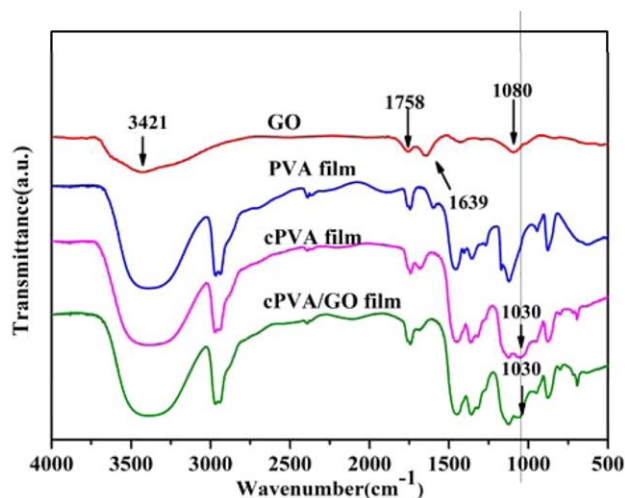


Figure 5. FTIR spectra of GO, PVA film, cPVA film, and cPVA/GO film. [Color figure can be viewed in the online issue, which is available at wileyonlinelibrary.com.]

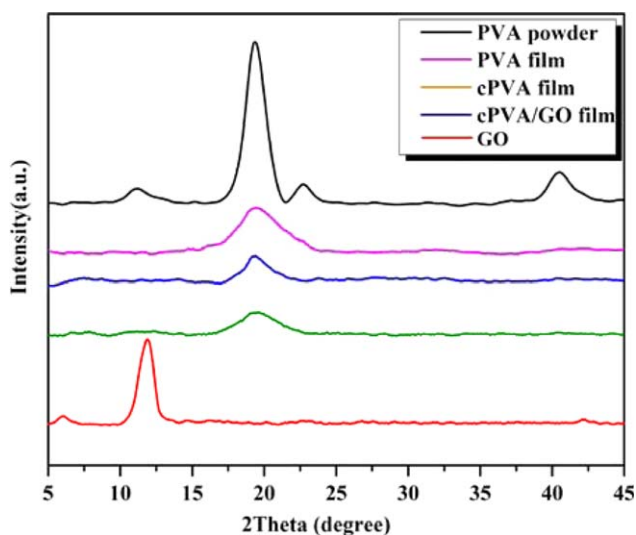


Figure 6. XRD patterns of PVA powder, PVA film, cPVA film, cPVA/GO film, and GO. [Color figure can be viewed in the online issue, which is available at wileyonlinelibrary.com.]

The FTIR spectrum of cPVA/GO (with GO content 0.5 wt %) seems to be similar to that of cPVA. However, there are also studies that suggest the existence of GO would have an effect on the FTIR spectrum of PVA. Wang *et al.*'s work³¹ pointed out that the C–O stretching peaks (1000–1200 cm^{-1}) of GO/PVA became very weak compared with that of pure PVA, suggesting the presence of interactions between the PVA and GO. In Bao *et al.*'s study,³² it was noticed that ν O–H wavenumbers in the PVA nanocomposites moved to smaller wavenumbers compared with neat PVA, and it was assumed to be ascribed to the dissociation of the hydrogen bond among the hydroxyl groups in PVA molecules. Moreover, a reduction of hydrogen bonds among the PVA matrix was observed by them when GO was added into PVA, which was probably due to the incorporation of GO sheets cutting off the hydrogen bond between the PVA molecules. But in this work, the addition of GO didn't lead to an obvious change of the FTIR spectrum of cPVA, which can also be explained that the effect of GO is weakened by boric acid added first.

XRD Analysis

XRD was performed to confirm the phase composition and microstructure of the materials and prepared films. As it is shown in Figure 6, the PVA powder used in this work has three diffraction peaks at $2\theta = 19.8^\circ$, 22.9° , and 40.6° , which correspond to the characteristic peaks of PVA.³³ However, the PVA films (no matter crosslinked or not) that prepared from the PVA solution show only one peak at $2\theta = 19.8^\circ$. What's more, such a peak does not make any shifts but the relative intensity decreases when BA was added, suggesting the decrease of the crystallinity and the existence of interactions between the polymer chains and BA. The effect of GO on the crystallinity of PVA seems to be very little since the peak (at 19.8°) of cPVA/GO does not show resolvable difference from that of cPVA films, which is also noticed in the previous literature.³⁴ The characteristic peak of GO sheets appears at $2\theta = 12^\circ$. From the Bragg equation ($2d\sin\theta = n\lambda$) it can be calculated that the

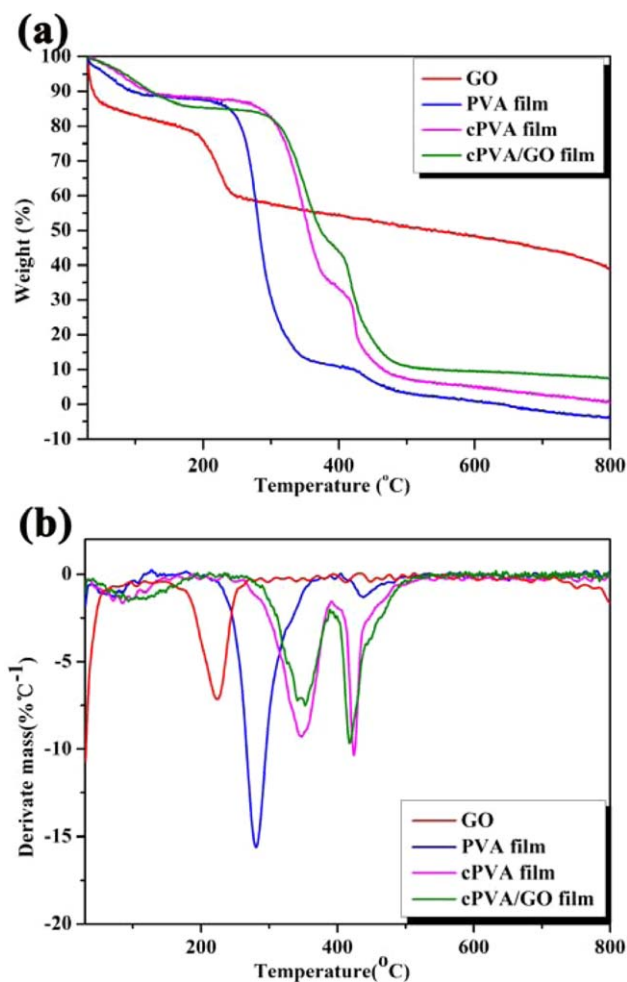


Figure 7. TGA (a) and DTG (b) curves of GO, PVA film, cPVA film, and cPVA/GO film. [Color figure can be viewed in the online issue, which is available at wileyonlinelibrary.com.]

interlayer distance of GO is 0.6 nm. After GO is dispersed into the PVA matrix, the XRD patterns of the cGO/PVA films only show the PVA diffraction peak, and the characteristic diffraction peak of GO disappears. This result demonstrates that GO is fully exfoliated into single GO sheet in the PVA matrix.³²

Thermal Stability

Figure 7 gives the thermo gravimetric analysis (TGA) and corresponding DTA results for GO, pure PVA, cPVA, and cPVA/GO film with 0.5 wt % GO loading, respectively. All the PVA films (no matter crosslinked or reinforced by GO) decompose in a similar process: the first loss (about 10%) takes place before 200°C, which is mainly ascribed to the removal of adsorbed water and decomposition of labile oxygen functional groups in the material; the main loss over the temperature range of 200–450°C is 50–70%, which can be assigned to the thermal decomposition of the PVA matrix. What is more, the TGA curves of the cPVA as well as the cPVA/GO films are shifted toward a higher temperature when compared to that of pure PVA. As it shows in Figure 7, the onset temperatures of pure PVA, cPVA, and cPVA/GO films to decompose rapidly are about 230, 280,

310°C respectively, which means that both BA and GO can significantly improve the thermal stability of PVA films.

It is known that PVA is a semicrystalline polymer in which high physical interactions between the polymer chains exist due to hydrogen bonding between the hydroxyl groups. The introduction of a crosslinking agent (in this work, boric acid) affects both crystallinity and physical network, originating variations in the T_g values of the system. Generally, the mechanical and thermal properties would suffer a decrease since the crosslinking reaction can cause a diminution of crystallinity of the system. But the result of this work shows a different phenomenon. The reasons of this behavior is explained as a result of the competitive action of three factors during the crosslinking: (1) decrease of the existing physical network due to the reduction of hydrogen bonding, which would cause a damage to the thermal stability; (2) formation of a chemical network, which would enhance the thermal stability; and (3) introduction of moieties due to the specific chemical structure of the crosslinker itself, the effect of which might depend on the chemical and physical properties of the crosslinker.² In this work, a BA reacts with the diol unit of PVA to form a stable five-membered ring, and this rigid chemical structure could bring about benefit to the thermal stability of PVA films.

As for GO, from Figure 7, we can find that it is not thermally stable and starts to lose mass sharply upon heating even below 50°C, and another decrease of weight follows at the temperature around 200°C. This may be due to the large number of oxygen-containing functional groups such as hydroxyls, carboxyls and epoxides on the GO sheets, since these groups are not thermally stable and easy to absorb water.^{31,32} When the water and thermally labile oxygen functional groups are removed, the thermal stability of GO is improved. So, a slow decline shows up after 200°C, and the total mass maintains at a relatively high level. The further T_g increase of the cPVA/GO can be explained that the polymer chains are constrained by the chemical bond interaction, i.e., the hydrogen bonding reaction, between the hydroxyl groups of the PVA chains with the oxygen-containing groups of the GO sheets. The bonding is expected to affect the mobility of PVA chains, and the thermal stability is improved as result. In addition, Wang *et al.* suggested other two possible factors that might determine the thermal stability: (1) GO acted as gas barriers suppressing the decomposition of PVA, leading to increased decomposition temperature. (2) CO, CO₂, and H₂O released during reduction around 200°C might accelerate the decomposition of PVA.³⁵

Mechanical Properties

As it is showed in Figure 8, the tensile strength of PVA films increases sharply (from 23.28 ± 2.39 to 60.43 ± 4.79 Mpa) when 2 wt % BA is added as crosslinking agent. However, as the content of BA increases, the increment of tensile strength is not dramatic. The strength reaches its maximum (76.24 ± 5.97 MPa) when the mass ratio of BA is 10 wt %, then it has a slight reduction as the BA content increases to 15 wt %. On the other hand, the ductility which is characterized by the elongation at break decreases remarkably with the increase of BA content. It can be explained that, through the reaction of PVA and BA, the

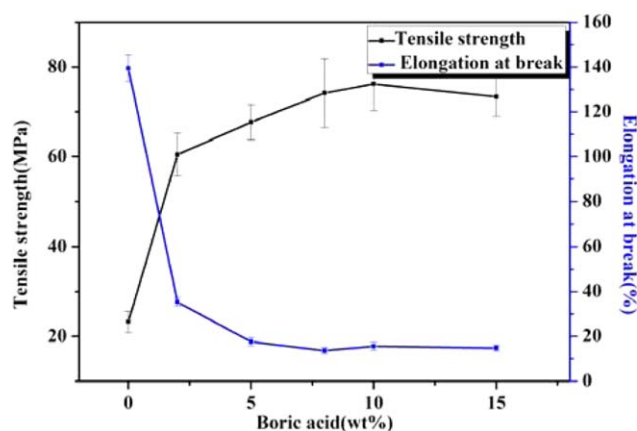


Figure 8. Tensile stress and elongation at break of cPVA films with various BA content. [Color figure can be viewed in the online issue, which is available at wileyonlinelibrary.com.]

hydroxyls ($-\text{OH}$ s) from different PVA chains crosslink with each other, which restricts the mobility of PVA units. Therefore, the tensile strength is improved for the strong bonds formed by BA and the elongation at break decreases for the same reason.

Figure 9 shows the tensile strengths and elongations at break of (a) PVA/GO and (b) cPVA/GO films as a function of GO load-

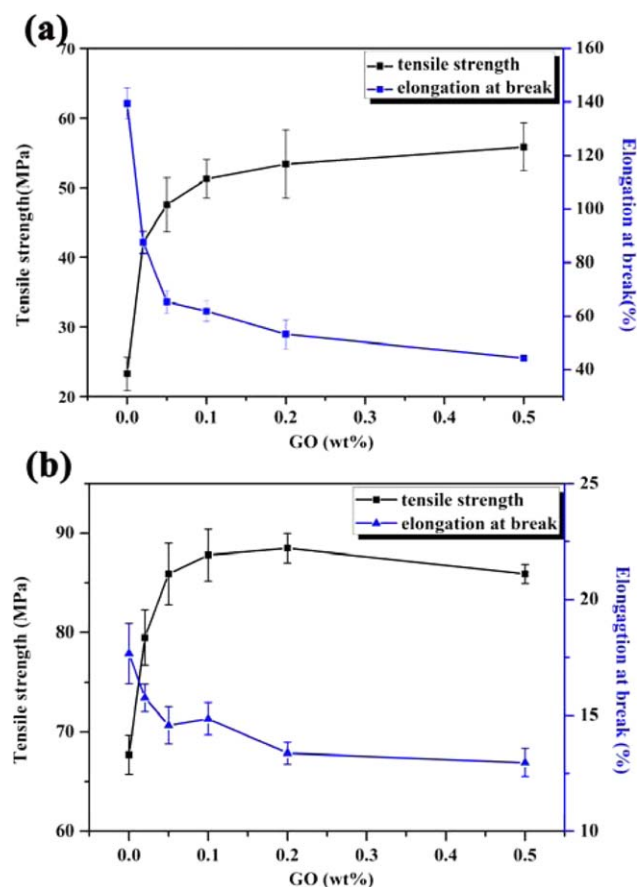


Figure 9. Tensile strength and elongation at break of (a) PVA/GO and (b) cPVA/GO films as a function of GO loadings, respectively. [Color figure can be viewed in the online issue, which is available at wileyonlinelibrary.com.]

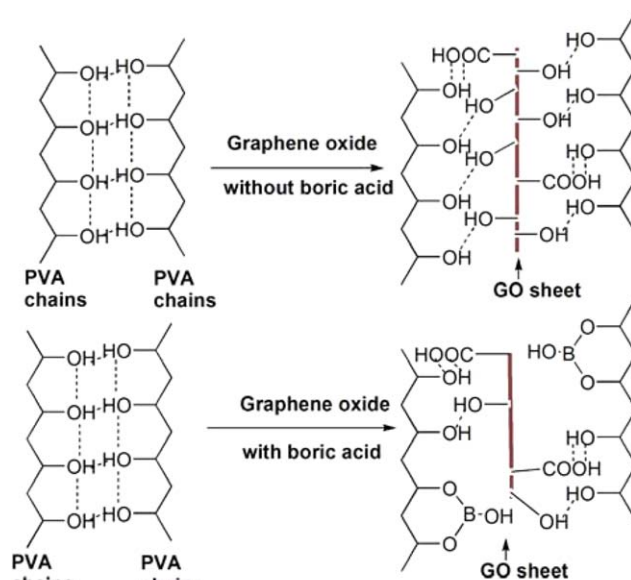


Figure 10. Illustration of hydrogen bonding interaction among PVA and GO. [Color figure can be viewed in the online issue, which is available at wileyonlinelibrary.com.]

ings respectively. All films in Figure 9(b) were crosslinked with 5 wt % BA, which exhibits a similar tendency with the curve in Figure 8, that is, with the increase of GO loading, the tensile strength of cPVA/GO films presents an inverted U-shape (reaches the maximum of 88.5 MPa at 0.2 wt %), which is a little different from the Figure 9(a), since the tensile strength showed in Figure 9(a) continually increases as the GO content rises. Figure 9(a) reflects a common tendency that the PVA/GO composite usually has. For example, the research of Xiaodong Qi's group found that, the tensile strength of PVA/GO showed a continuous increment even the GO content increased to 1.0 wt %.³⁶ Similar result was reported by Xu *et al.*³⁷ which indicated that the GO sheets could further enhance the tensile strength of PVA/GO film at a concentration of 3 wt %. However, in Figure 9(b), the maximum ratio of GO is 0.5 wt %, which is relatively lower than the content mentioned above. What's more, the strength increment of cPVA/GO declines when BA was used compared to the PVA/GO films. For example, 0.02 wt % GO brings about a growth of about 12 MPa in cPVA/GO group while the corresponding specimen in PVA/GO group exhibits an increase of 20 MPa.

The possible reason that causes this abnormal phenomenon is given in Figure 10.^{22,36} During the preparation of the cPVA/GO films, the oxygenated functionalities (hydroxyl, carboxylic groups) of GO are linked with the hydroxyl groups of the PVA via the formation of hydrogen bonding. Therefore, when certain amount of BA (in this paper, 5 wt %) is added as crosslinking agent, a large proportion of hydroxyl groups ($-\text{OH}$ s) link with BA, and the left part of hydroxyl groups form a decreasing amount of hydrogen bonding with GO sheets. Although there is also other combination such as mechanical connection between GO sheets and PVA matrix, in this case, hydrogen bonding plays a leading role.

Table I. Tensile Strength of GO Reinforced PVA Composites

Fraction of GO (wt %)	Preparation method	Increase of tensile strength (%)	References
0.02	Electrostatic spinning	4200	35
0.5	Solvent casting	212	31
0.8	Solvent casting	66	32
3	Vacuum filtration	69	37
0.2	Solvent casting	31	This work

Another probable reason leading to this difference is the inhomogeneity of the cPVA/GO films caused by the high viscosity of the PVA solution, especially when 5 wt % BA is added. The nonuniformity of the thickness often causes a fracture at the relatively thin part, which may decrease the final tensile strength.

As a result, the addition of GO sheets does not lead to a considerable improvement of tensile strength of cPVA/GO films, which can be confirmed by the studies listed in Table I.

However, it is an undeniable fact that both mechanical performance and thermal stability are improved to some extent by the incorporation of GO sheets even the crosslinking agent is used.

Fracture Morphology of cPVA/GO Film

Figure 11 shows the SEM images of the fracture surface of cPVA (a) and cPVA/0.5 wt % GO (b) film after tensile testing. As shown in Figure 11(b), the fracture surface of the composite film exhibits a rough layered structure just as reported previously,³⁸ while the fracture surface of cPVA film is much smoother. It was suggested that the plate-like GO sheets could present preferential orientation within the film and tend to align parallel to the film surface, thus resulting in the formation of a layered like structure. It's interesting to notice that, at the fracture surface, there is no evident presence of GO sheet. But

such laminar structure indicates that GO sheets are wrapped with the PVA matrix and the presence of strong combination between GO and PVA.³⁷

CONCLUSIONS

In this work, the effect of BA and GO on the mechanical property and thermal stability of PVA film was explored, and the main conclusions are summarized as follows. (1) Both BA and GO can improve the mechanical and thermal properties of PVA film: 5 wt % boric acid could increase the tensile strength three-fold (from 23.3 to 67.7 MPa), and 0.5 wt % GO alone could improve the tensile strength from 23.3 to 53.4 MPa. The combination of 5 wt % BA and 0.2 wt % GO can provide an enhancement of about 65 to 88.5 MPa. Moreover, the decomposition temperature was increased by about 50 to 280°C with the addition of 5 wt % BA and was further improved to nearly 310°C when 0.5 wt % GO was added simultaneously. (2) However, in the case of tensile strength, it seems that the existence of BA would weaken the enhancement of the following GO sheets, and even causes a decline of the tensile strength when the GO content is more than 0.2 wt %, since both these two components share a similar reinforcement mechanism: through the reaction with the hydroxyl of PVA.

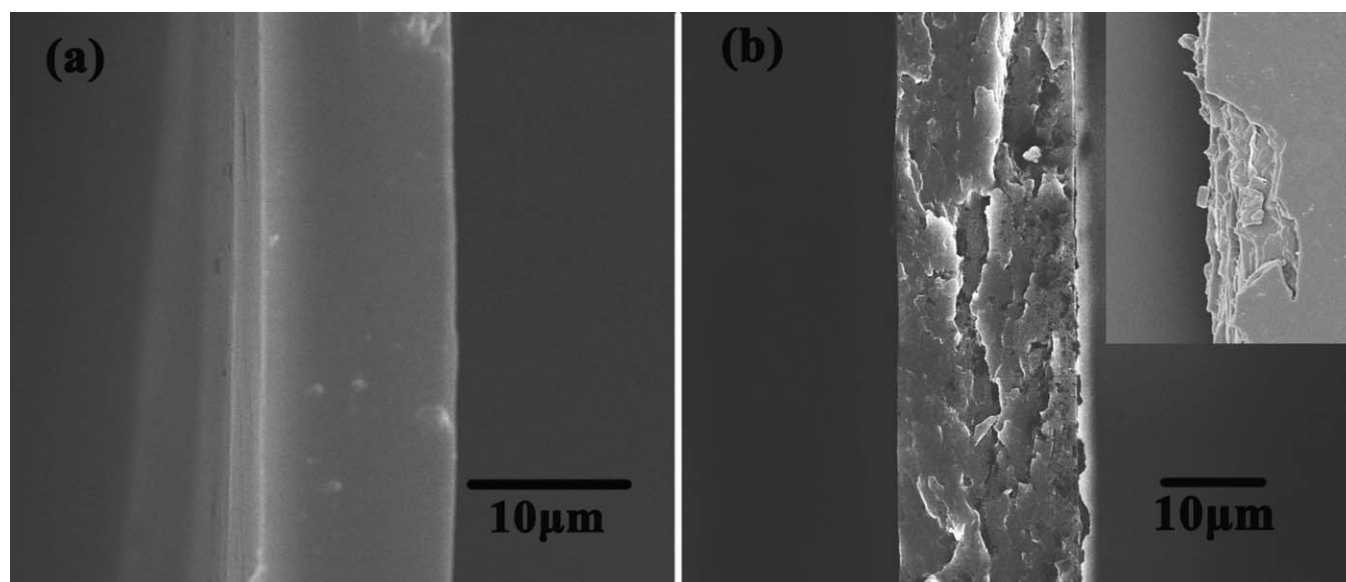


Figure 11. SEM images of fracture surface of (a) cPVA, (b) cPVA/0.5 wt % GO film (the inset picture shows the surface from horizontal perspective).

REFERENCES

1. Baker, M. I.; Walsh, S. P.; Schwartz, Z.; Boyan, B. D. *J. Biomed. Mater. Res. Part B* **2012**, *100B*, 1451.
2. Krumova, M.; Lopez, D.; Benavente, R.; Mijangos, C.; Perena, J. M. *Polymer* **2000**, *41*, 9265.
3. Yeom, C. K.; Lee, K. H. *J. Membr. Sci.* **1996**, *109*, 257.
4. Gough, J. E.; Scotchford, C. A.; Downes, S. J. *Biomed. Mater. Res.* **2002**, *61*, 121.
5. Kim, D. S.; Park, H. B.; Rhim, J. W.; Lee, Y. M. *J. Membr. Sci.* **2004**, *240*, 37.
6. Dzondo-Gadet, M.; Mayap-Nzietchueng, R.; Hess, K.; Nabet, P.; Belleville, F.; Dousset, B. *Biol. Trace Elem. Res.* **2002**, *85*, 23.
7. Hakki, S. S.; Dundar, N.; Kayis, S. A.; Hakki, E. E.; Hamurcu, M.; Kerimoglu, U.; Baspinar, N.; Basoglu, A.; Nielsen, F. H. *J. Trace Elem. Med. Biol.* **2013**, *27*, 148.
8. Hakki, S. S.; Bozkurt, B. S.; Hakki, E. E. *J. Trace Elem. Med. Biol.* **2010**, *24*, 243.
9. Hunt, C. D. *J. Trace Elem. Med. Biol.* **2012**, *26*, 157.
10. Nielsen, F. H. *Biofactors* **2004**, *20*, 161.
11. Meacham, S. L.; Taper, L. J.; Volpe, S. L. *Environ. Health Perspect.* **1994**, *102*, 79.
12. Naghii, M. R.; Torkaman, G.; Mofid, M. *Biofactors* **2006**, *28*, 195.
13. Watcharotone, S.; Dikin, D. A.; Stankovich, S.; Piner, R.; Jung, I.; Dommett, G. H. B.; Evmenenko, G.; Wu, S. E.; Chen, S. F.; Liu, C. P.; Nguyen, S. T.; Ruoff, R. S. *Nano Lett.* **2007**, *7*, 1888.
14. Kuila, T.; Bose, S.; Khanra, P.; Mishra, A. K.; Kim, N. H.; Lee, J. H. *Biosens. Bioelectron.* **2011**, *26*, 4637.
15. Sun, X. M.; Liu, Z.; Welsher, K.; Robinson, J. T.; Goodwin, A.; Zaric, S.; Dai, H. *J. Nano Res.* **2008**, *1*, 203.
16. Wu, S.-D.; Lv, W.; Xu, J.; Han, D.; Chen, X.; Wang, P.; Yang, Q.-H. *J. Mater. Chem.* **2012**, *22*, 17204.
17. Sheikh, F. A.; Barakat, N. A. M.; Kanjwal, M. A.; Park, S. J.; Park, D. K.; Kim, H. Y. *Macromol. Res.* **2010**, *18*, 59.
18. Zhao, X.; Zhang, Q.; Chen, D.; Lu, P. *Macromolecules* **2010**, *43*, 2357.
19. Potts, J. R.; Dreyer, D. R.; Bielawski, C. W.; Ruoff, R. S. *Polymer* **2011**, *52*, 5.
20. Huang, Y.; Han, S.; Pang, X.; Ding, Q.; Yan, Y. *Appl. Surf. Sci.* **2013**, *271*, 299.
21. Nielsen, F. *Plant Soil* **1997**, *193*, 199.
22. Dreyer, D. R.; Park, S.; Bielawski, C. W.; Ruoff, R. S. *Chem. Soc. Rev.* **2010**, *39*, 228.
23. Şenel, M.; Bozkurt, A.; Baykal, A. *Ionics* **2007**, *13*, 263.
24. Zhao, D. C.; Zhang, D.; Zhang, M.; Zhang, R. W.; Gao, G.; Song, X. M.; Li, Y.; Li, Q.; Liu, F. Q. *Abstr. Pap. Am. Chem. S* **2005**, 229, U948.
25. Wang, H. H.; Shyr, T. W.; Hu, M. S. *J. Appl. Polym. Sci.* **1999**, *74*, 3046.
26. Yildirim, M.; Fischer, H.; Marx, R.; Edelhoff, D. *J. Prosthet. Dent.* **2003**, *90*, 325.
27. Cheng, A. T. Y.; Rodriguez, F. *J. Appl. Polym. Sci.* **1981**, *26*, 3895.
28. Viswanath, B.; Ravishankar, N. *Script. Mater.* **2006**, *55*, 863.
29. Mondal, S.; Banthia, A. K. *J. Eur. Ceram. Soc.* **2005**, *25*, 287.
30. Barros, P. M.; Yoshida, I. V. P.; Schiavon, M. A. *J. Non-Crystallogr. Solids* **2006**, *352*, 3444.
31. Wang, J.; Wang, X.; Xu, C.; Zhang, M.; Shang, X. *Polym. Int.* **2011**, *60*, 816.
32. Bao, C.; Guo, Y.; Song, L.; Hu, Y. *J. Mater. Chem.* **2011**, *21*, 13942.
33. García-Cerda, L. A.; Escareno-Castro, M. U.; Salazar-Zertuche, M. *J. Non-Crystallogr. Solids* **2007**, *353*, 80.
34. Zhang, L.; Wang, Z.; Xu, C.; Li, Y.; Gao, J.; Wang, W.; Liu, Y. *J. Mater. Chem.* **2011**, *21*, 10399.
35. Wang, C.; Li, Y.; Ding, G.; Xie, X.; Jiang, M. *J. Appl. Polym. Sci.* **2013**, *127*, 3026.
36. Qi, X.; Yao, X.; Deng, S.; Zhou, T.; Fu, Q. *J. Mater. Chem. A* **2014**, *2*, 2240.
37. Xu, Y. X.; Hong, W. J.; Bai, H.; Li, C.; Shi, G. Q. *Carbon* **2009**, *47*, 3538.
38. Yang, X. M.; Li, L. A.; Shang, S. M.; Tao, X. M. *Polymer* **2010**, *51*, 3431.